ChemPubSoc Europe

DOI: 10.1002/chem.201402978

CHEMISTRY A European Journal Full Paper

Hydrogenation

A Theoretically-Guided Optimization of a New Family of Modular P,S-Ligands for Iridium-Catalyzed Hydrogenation of Minimally Functionalized Olefins

Jèssica Margalef,[a] Xisco Caldentey,[b] Erik A. Karlsson,[b] Mercè Coll,[a] Javier Mazuela,[a] Oscar Pàmies,[a] Montserrat Diéguez,*[a] and Miquel A. Pericàs*[b, c]

Abstract: A library of modular iridium complexes derived from thioether-phosphite/phosphinite ligands has been evaluated in the asymmetric iridium-catalyzed hydrogenation of minimally functionalized olefins. The modular ligand design has been shown to be crucial in finding highly selective catalysts for each substrate. A DFT study of the transition state responsible for the enantiocontrol in the Ir-catalyzed hydrogenation is also described and used for further optimization of the crucial stereodefining moieties. Excellent enantioselectivities (enantiomeric excess (*ee*) values up to 99%) have been obtained for a range of substrates, including *E*- and *Z*-trisubstituted and disubstituted olefins, α,β-unsaturated enones, tri- and disubstituted alkenylboronic esters, and olefins with trifluoromethyl substituents.

Introduction

The growing demand for enantiomerically pure products, required in the preparation of both compounds of technological interest and compounds possessing biological activity, has stimulated the search for highly efficient asymmetric catalytic processes that display high selectivity and activity, minimal consumption of energy, and minimal generation of byproducts.[1] Compared with other techniques, asymmetric catalysis is an attractive strategy because it uses only a small amount of catalyst to produce an extensive amount of the requested target compound, thus reducing the formation of byproducts. It also has the advantage of reducing the number of reaction steps and synthetic operations, thus bringing down the overall production cost.[1]

Asymmetric hydrogenation has become a highly useful tool for preparing enantiomerically pure compounds because of its high efficiency, low catalyst loadings, operational simplicity, and perfect atom economy.[1–2] Its uses have been largely accepted by the chemical community as illustrated by the commercial production of the Parkinson's drug L-3,4-dihydroxyphenylalanine (L-DOPA),[3] the broad-spectrum antibiotic levofloxacin (Daichii-Sankyo Co.),[4] and sitagliptin (Merck),[5] as well as the synthesis of the pesticide (*S*)-metolachlor.[6] Whereas today a notable series of chiral ligands (mostly phosphorus-based) for the Ru- and Rh-catalyzed hydrogenation of olefins possessing polar functional groups is available to the chemical community,[2a,b] the reduction of minimally functionalized substrates is by far less well-developed.[2d,7] The use of chiral analogues of Crabtree's catalyst[8] modified with phosphine-oxazoline (PHOX) ligands ([Ir(PHOX)(cod)][BAr_F]) (cod = 1,5-cyclooctadiene; [BAr_F] = [B{3,5-$(CF_3)_2C_6H_3$}$_4$]$^-$) represented the first breakthrough in the hydrogenation of this type of substrate.[9] Since then, mixed phosphorus-oxazoline ligands have been the most popular heterodonor ligands in this process. Many successful P-oxazoline ligands have been prepared by incorporating P-donor groups other than phosphines and by modifying the chiral backbone.[10] Although these modifications have aided the development of new ligands that have considerably expanded the scope of Ir-catalyzed hydrogenation, most of the screened catalysts are still highly substrate-dependent, and their preparation involves long synthetic sequences. The development of efficient modular chiral ligands, readily available from simple starting materials, which tolerate a broad range of substrates, still remains a challenge. More recently, research has been expanded to design heterodonor P,X-ligands bearing more robust X-donor groups than oxazolines (pyridines,[11] amides,[12] thiazoles,[13] oxazoles,[14] etc.). In this respect, we have recently described the successful use of non-*N*-donor heterodonor ligands, sugar-based thioether-phosphorus ligands, for enantioselective Ir-catalyzed reduction of minimally functionalized olefins.[15] Ir-complexes modified with these P-thioether ligands efficiently catalyzed the hydrogenation of a large range of *E*- and *Z*-trisubstituted olefins and the more

[a] J. Margalef, Dr. M. Coll, Dr. J. Mazuela, Dr. O. Pàmies, Prof. M. Diéguez
Departament de Química Física i Inorgànica, Universitat Rovira i Virgili
C/Marcel·li Domingo, s/n., 43007 Tarragona (Spain)
E-mail: montserrat.dieguez@urv.cat

[b] Dr. X. Caldentey, Dr. E. A. Karlsson, Prof. M. A. Pericàs
Institute of Chemical Research of Catalonia (ICIQ)
Av. Països Catalans, 16, 43007 Tarragona (Spain)
E-mail: mapericas@iciq.es

[c] Prof. M. A. Pericàs
Departament de Química Orgànica
Universitat de Barcelona, 08028 Barcelona (Spain)

Supporting information for this article is available on the WWW under http://dx.doi.org/10.1002/chem.201402978.

difficult disubstituted olefins. The results are comparable to the best ones reported in the literature. Apart from this, the use of other phosphorus-thioether ligands in the same process remains unexplored, and a systematic study of the scope of P,S-ligands is still needed. No mechanistic studies have been made using this type of ligands to enable a priori prediction of the right ligand needed to obtain high enantioselectivity. Therefore, more research is needed to discern the role of ligand parameters in the origin of enantioselectivity.

To address all these points, in this study we have prepared and evaluated a new highly modular thioether-phosphite/phosphinite ligand library (Figure 1) in the Ir-catalyzed hydrogenation of a broad range of minimally functionalized olefins, including examples with neighboring polar groups. These ligands are easily prepared in few steps from readily available enantiopure arylglycidols. They also incorporate the advantages of the robustness of the thioether moiety[16] and the additional control provided by the flexibility of the chiral pocket through a highly modular ligand scaffold. In a simple three step procedure (Scheme 1), several ligand parameters could easily be tuned to maximize the catalyst performance. With this ligand library, we therefore investigated the effect of systematically changing the thioether (**L1**–**L6**) and alkoxy (**L1**, **L7**, and **L9**) groups, the nature of the starting material arylglycidol (**L10**), the configuration of the biaryl phosphite moiety (**a**–**c**), and the consequences of replacing the phosphite moiety by a phosphinite group (**d**–**g**). In this paper we have also carried out DFT calculations to explain the origin of enantioselectivity. These DFT calculations have also been crucial in the optimization of the ligand design. Interestingly, we found that the catalytic performance of the new ligands is excellent and similar to the performance of the previous furanoside thioether-phosphorus counterparts,[15] which have recently emerged as some of the most successful catalysts designed for this process, with two added advantages. First, these new Ir-thioether-P catalytic systems are able to expand the scope to a larger range of olefins, which includes α,β-unsaturated enones, tri- and disubstituted alkenylboronic esters and olefins with trifluoromethyl substituents. Second, since the starting enantiopure epoxides are prepared through a catalytic Sharpless epoxidation, both enantiomeric series of the target P,S-ligands are equally available. The potential applicability of the Ir-thioether-phosphite/phosphinite catalyst precursors ([Ir(cod)(**L1**–**L10a**–**g**)][BAr_F]) was further proved using propylene carbonate as a green alternative solvent, which allows catalyst recycling.

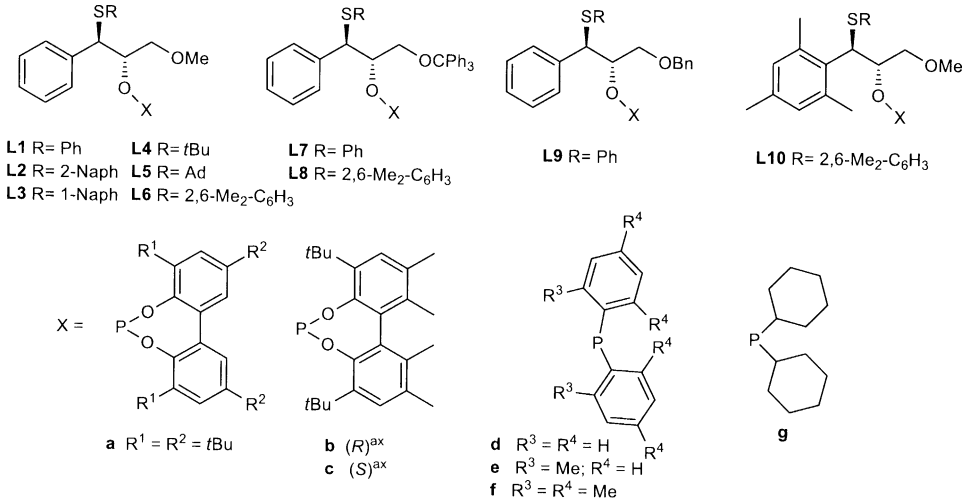

Figure 1. Thioether-phosphite/phosphinite ligand library **L1**–**L10a**–**g**.

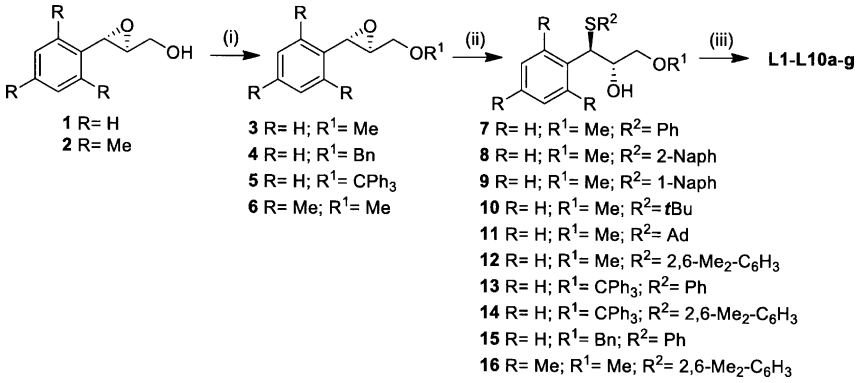

Scheme 1. Synthesis of new thioether-phosphite/phosphinite ligands **L1**–**L10a**--**g**. i) R^1X/NaH/DMF;[18] ii) R^2SH/NaOH/dioxane/H_2O;[17] iii) $ClP(OR)_2$/pyridine/toluene/80 °C or $ClPR_2$/NEt_3/toluene.

Results and Discussion

Synthesis of ligands

The new thioether-phosphite **L1**–**L10a**–**c** and phosphinite **L1**–**L10d**--**g**[17] ligands were efficiently synthesized in one step from the corresponding readily accessible thioether-alcohols (**7**–**16**; Scheme 1). These compounds are easily prepared in two steps from enantiopure arylglycidols readily available on a large scale (0.5–1.0 mol)[18] following previously reported procedures.[17] In the first step, the protection of the free hydroxyl group enables us to introduce the desired variety in the alkoxy group (Scheme 1, step i).[18c] In the second step, the regioselec-

tive and stereospecific ring opening by thiolates produced the corresponding thioether-hydroxyls (**7**–**16**; Scheme 1, step ii), thus giving room for additional diversity by performing the opening with different thiolates.[17] The last step of the ligand synthesis (Scheme 1, step iii) is the reaction of the corresponding thioether-hydroxyl in the presence of base with one equivalent of either the corresponding biaryl phosphorochloridite ($ClP(OR)_2$; $P(OR)_2$ = **a**–**c**) to provide thioether-phosphite ligands (**L1**–**L10 a**–**c**) or the required chlorophosphine ($ClPR_2$; PR_2 = **d**–**g**) to achieve the new thioether-phosphinite ligands (**L1**–**L10 d**–**g** (Scheme 1, step iii).

All of the ligands are stable in air at room temperature and to hydrolysis. They were isolated in good yields as white solids or colorless oils after purification on neutral alumina.

Synthesis of the Ir-catalyst precursors

The catalyst precursors were prepared by treating $[Ir(\mu\text{-}Cl)(cod)]_2$ (0.5 equiv) with an equimolar amount of the appropriate P,S-ligand (**L1**–**L10 a**–**g**) in dichloromethane at reflux for 1 h. The Cl^-/BAr_F^- counterion exchange was then performed by reaction with sodium tetrakis[3,5-bis(trifluoromethyl)phenyl]borate ($NaBAr_F$; 1 equiv) in water (Scheme 2). The catalyst precursors were obtained in pure form as air-stable red-orange solids. No further purification was thus needed. It should be mentioned that all attempts to prepare iridium complexes containing thioether-phosphinite ligands with the extremely bulky mesityl phosphinite (**f**) moiety were unsuccessful.

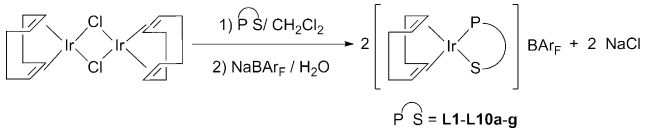

Scheme 2. Synthesis of Ir precursors [Ir(cod)(P–S)][BAr_F] (P–S = **L1**–**L10 a**–**g**).

The HRMS-ESI spectra show the heaviest ions at *m*/*z*, which correspond to the loss of the BAr_F anion from the molecular species. The complexes were also characterized by ^1H, ^{13}C, and ^{31}P NMR spectroscopy. The spectral assignments, made using ^1H-^1H and ^{13}C-^1H correlation measurements, were as expected for these C_1-symmetric iridium complexes.

Variable-temperature (VT)-NMR spectroscopic experiments in CD_2Cl_2 (+35 to −85 °C) indicate the presence of a single isomer in all cases except for [Ir(cod)(**L1**–**L9 a**)][BAr_F] compounds. For these latter complexes, the ^{31}P VT-NMR spectra show that the signals become broader when the temperature is lowered. This behavior could indicate a rapid exchange of the possible diastereoisomers formed by conformational isomerism of the biphenyl moiety and/or when the thioether coordinates to the metal atom. The fact that the presence of different diastereoisomers in solution is only observed for complexes with ligands containing a conformationally labile biphenyl moiety (**a**) and not for related complexes with ligands containing enantiopure biphenyl moieties (**b**,**c**), suggests that this behavior is due to the fast exchange of the biphenyl moiety on the NMR timescale. This hypothesis is further confirmed in the X-ray analysis of [Ir(cod)(**L6 a**)][BAr_F], which shows the presence of the two diastereoisomers resulting from the conformational isomerism of the biphenyl phosphite moiety in the solid state (see the Supporting Information). All this indicates that the ligand backbone is not able to control the conformational isomerism of the biaryl phosphite group. Therefore, it is not surprising that in catalytic studies the enantioselectivity obtained with [Ir(cod)(**L1**–**L9 a**)][BAr_F] precursors was low (see below). It could thus be concluded from the VT-NMR experiments that the catalyst precursors are configurationally stable in solution at the sulfur center, which, however, does not necessarily imply that the same holds true for the catalytically active Ir^{III}/Ir^{V} complexes during the reaction conditions (see below).

Crystals suitable for X-ray diffraction analysis of [Ir(cod)(**L1 d**)][BAr_F], [Ir(cod)(**L4 a**)][BAr_F], and [Ir(cod)(**L9 a**)][BAr_F] complexes were also obtained to determine the coordination mode of this new ligand class (Figure 2). In contrast to Ir-**L6 a** complex, the solid-state structure of complexes containing **L4 a** and **L9 a** indicated that only one of the diastereoisomers crystallized.

In all cases, the six-membered chelate ring adopted a chair conformation, with the alkoxide group pointing in the opposite direction to the coordination sphere. However, whereas the crystal structures of [Ir(cod)(**L**)][BAr_F] (**L** = **L4 a**, **L6 a**, and **L9 a**), containing a phosphite moiety, showed the thioether substituent in an equatorial position, an axial disposition of the thioether substituent was observed for [Ir(cod)(**L1 d**)][BAr_F], containing a phosphinite group.

Asymmetric hydrogenation

Asymmetric hydrogenation of the minimally functionalized model olefin E-2-(4-methoxyphenyl)-2-butene (S1): A computational study for ligand optimization

Initially, we applied phenylglycidol-based ligands **L1**–**L9 a**–**g** in the Ir-catalyzed hydrogenation of the model substrate *E*-2-(4-methoxyphenyl)-2-butene (**S1**). Model substrate **S1** has been successfully reduced by a large number of catalysts, thus enabling a direct comparison of the potential of the new ligands with the state of the art.[2d,7] The results, which are summarized in Table 1, indicated that the enantioselectivity is mainly affected by the thioether substituent and the type of P-donor group, whereas the effect of the alkoxy substituent is less pronounced. The small effect of the alkoxy substituent on enantioselectivity (i.e., Table 1; entries 1, 24, and 32) is not unexpected since this substituent is located far away from the coordination sphere as can be seen in the X-ray structures (see above) and the DFT-calculated transition states (TS; see below).

We found that the correct choice of the thioether substituent is crucial to achieve the highest levels of enantioselectivity. The results showed that the presence of aryl substituents provided higher enantioselectivities than alkyl thioether substituents. Among the aryl substituents, enantioselectivities increase with increasing steric bulk of the thioether substituent (2,6-

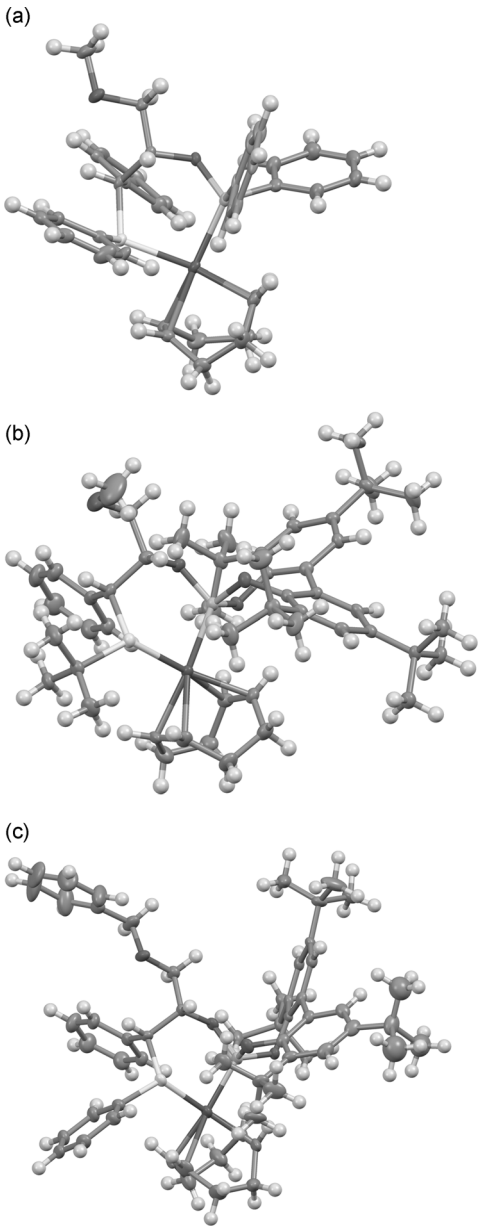

Figure 2. X-ray structures of: a) [Ir(cod)(**L1 d**)][BAr_F] (CCDC-993594); b) [Ir(cod)(**L4 a**)][BAr_F] (CCDC-993595), and c) [Ir(cod)(**L9 a**)][BAr_F] (CCDC-993597) (the BAr_F^- counterion and solvent molecules have been omitted for clarity). These data can be obtained free of charge from The Cambridge Crystallographic Data Centre via www.ccdc.cam.ac.uk/data_request/cif.

Table 1. Results for the Ir-catalyzed hydrogenation of **S1** using the P,S-ligand library **L1**–**L9 a**–**g**.[a]

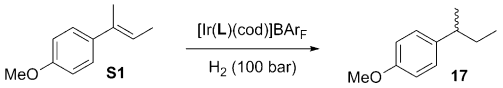

Entry	Ligand	*ee*[b] [%]	Entry	Ligand	*ee*[b] [%]
1	**L1 a**	26 (*R*)	19	**L6 a**	26 (*R*)
2	**L1 b**	42 (*R*)	20	**L6 b**	48 (*R*)
3	**L1 c**	13 (*R*)	21	**L6 c**	55 (*S*)
4	**L1 d**	44 (*R*)	22	**L6 d**	64 (*R*)
5	**L2 b**	40 (*R*)	23	**L6 e**	92 (*R*)
6	**L2 c**	12 (*R*)	24	**L7 a**	30 (*R*)
7	**L2 e**	84 (*R*)	25	**L7 b**	50 (*R*)
8	**L3 a**	8 (*R*)	26	**L7 c**	17 (*S*)
9	**L3 b**	36 (*R*)	27	**L7 d**	41 (*R*)
10	**L3 c**	31 (*S*)	28	**L7 e**	86 (*R*)
11	**L3 e**	86 (*R*)	29	**L7 g**	8 (*R*)
12	**L4 a**	14 (*R*)	30	**L8 a**	24 (*R*)
13	**L4 b**	41 (*R*)	31	**L8 e**	93 (*R*)
14	**L4 c**	19 (*R*)	32	**L9 a**	31 (*R*)
15	**L4 d**	53 (*R*)	33	**L9 b**	45 (*R*)
16	**L4 e**	49 (*R*)	34	**L9 c**	34 (*R*)
17	**L5 a**	25 (*R*)	35	**L9 d**	41 (*R*)
18	**L5 e**	35 (*R*)	36[c]	**L8 e**	93 (*R*)

[a] Reactions carried out using 0.5 mmol of **S1**, 2 mol% of Ir-catalyst precursor, CH_2Cl_2 as solvent, 100 bar H_2, 4 h. Full conversions were achieved in all cases. [b] Enantiomeric excesses (*ee* values) determined by chiral GC. [c] Reaction carried out using 0.25 mol% of Ir-catalyst precursor for 8 h; 99% conversion.

Me_2-C_6H_3 > 1-Napth > 2-Napth > Ph; Table 1, entries 23, 11, 7, and 4).

Regarding the effect of the P-donor group on enantioselectivity, we found that the presence of a conformationally labile biaryl phosphite group (**a**) provided low enantioselectivities, because as observed in the VT-NMR spectra and X-ray structures of the [Ir(cod)(**L1**–**L9 a**)][BAr_F] catalyst precursors, the ligand backbone is not able to control its conformational isomerization (Table 1, entries 1, 8, 12, 17, 19, 24, 30, and 32). Enantioselectivities therefore increased by using enantiopure biaryl phosphite groups (**b**,**c**; that is, Table 1, entries 13 and 14 vs. 12). We also found that there is a cooperative effect between the configuration of the ligand backbone and the configuration of the biaryl group that led to a matched combination for ligands containing an *R*-biaryl phosphite moiety (**b**; Table 1, entries 13 and 14). However, the best enantioselectivities were obtained with ligands containing a phosphinite group (*ee* values up to 93%, Table 1, entry 31). In particular, replacing the phosphite moiety by a bulky di-*o*-tolyl phosphinite group had a positive effect on enantioselectivity, whereas the use of a cyclohexyl phosphinite group led to poor enantioselectivities (Table 1, entry 29). This behavior is in contrast with the negative effect observed when replacing the phosphite group by a phosphinite moiety in the previous furanoside-based thioether-P ligands.[15b] These results clearly show the importance of using a modular scaffold to build new ligand systems.

We also performed the reaction at low catalyst loading (0.25 mol%) using ligand **L8 e**. High enantioselectivity (93% *ee*) and activity were maintained.

With the aim to find which ligand parameters should be further modified to increase enantioselectivity, we performed a DFT computational study of the transition states involved in the enantiocontrol of the iridium-catalyzed hydrogenation of substrate **S1**. Several DFT studies using P,N- and carbene-N ligands have indicated that the hydrogenation of minimally functionalized alkenes proceeds via Ir^{III}/Ir^{V} tetrahydride intermediates.[10p,19] Recent studies by Hopmann and co-workers using a phosphine-oxazoline (PHOX)-based iridium catalyst,[19e] and by our group, in conjunction with the groups of Norrby and

Andersson, using Ir-phosphite-oxazoline ligands,[10p] strongly support that the hydrogenation of minimally functionalized olefins using P,N-ligands follows a mechanism involving an Ir^{III}/Ir^{V} migratory-insertion/reductive-elimination pathway (labeled 3/5-MI in Scheme 3). In these studies, two catalytic pathways were contemplated. The already mentioned 3/5-MI pathway and the mechanism involving an Ir^{III}/Ir^{V} σ-metathesis/reductive-elimination pathway (labeled 3/5-Meta in Scheme 3). It has also been shown that the transition states for the migratory-insertion in the 3/5-MI pathway ($\mathbf{TS_{MI}}$) and the σ-metathesis in the 3/5-Meta pathway ($\mathbf{TS_{META}}$) are responsible for the selectivity in the Ir-catalyzed hydrogenation, and that the enantioselectivity therefore could be reliably calculated from the relative energies of these transition states.[19d]

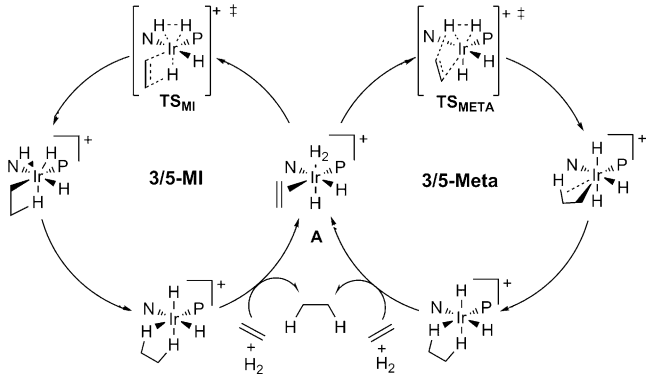

Scheme 3. 3/5-MI and 3/5-Meta catalytic cycles for the Ir-catalyzed hydrogenation.

On the basis of these previous studies we therefore performed a computational study of the $\mathbf{TS_{MI}}$ and $\mathbf{TS_{META}}$ transition states. To accelerate the DFT calculations, we initially studied ligands **L1 d** and **L6 d**, containing the simple unsubstituted diphenyl phosphinite moiety. In addition, these ligands contain two types of thioether groups that will help us to understand the already observed key role of introducing a bulky 2,6-dimethylphenyl thioether substituent on enantioselectivity. The transition states using **S1** as substrate for the stereochemistry determining migratory insertion ($\mathbf{TS_{MI}}$) or σ-bond metathesis ($\mathbf{TS_{META}}$) were calculated by using the B3LYP functional,[20] the 6-31G*/LANL2DZ basis set,[21] and the PCM solvent model with parameters for CH_2Cl_2,[22] as implemented in Gaussian 09.[23] The energies were further refined by performing single-point calculations at the 6-311 + G** level,[24] and by dispersion correction with the DFT-D3 model.[25]

Table 2 shows the calculated energies for the most stable isomers of the transition states ($\mathbf{TS_{MI}}$ and $\mathbf{TS_{META}}$). These key isomers are the result of varying between the two possible configurations at the sulfur center, coordinating to the two enantiotopic faces (*re* and *si*) of the olefin, and changing the relative position of the hydride (up or down).[26] It should be mentioned that olefins coordinated through the *si* face are reduced to the *R* product, whereas those coordinated through the *re* face give access to the *S* product. The results in Table 2 shows that the most stable transition state ($\mathbf{TSA1_{MI}}$) matches the major product obtained experimentally (*R* product, Table 1, entries 4 and 22), whereas the most stable transition state with the *re* face coordinated ($\mathbf{TSA8_{MI}}$) is expected to be responsible for the formation of the minor *S* product. The energy differences between the most stable transition states giving rise to the major and minor products are 4.5 and 8.5 kJ mol^{-1}, respectively, for **L1 d** and **L6 d**. We also found that the hydrogenation products are formed through the 3/5-MI mechanism, since the TS energies for the 3/5-Meta pathway, in both the major and minor configuration, are at least 13 kJ mol^{-1} higher than those for the 3/5-MI pathway (see Table 2). Nevertheless, since the energetic difference between the two pathways is relatively small, both have to be taken into consideration for further calculations. It should be pointed out that the fact that the calculations indicate that the minor *S* product is formed through a transition state in which the configuration at the sulfur center is *S*, whereas the major *R* product results from a transition state with *R* configuration at the sulfur center raised some concerns regarding the validity of the theoretical model. In general, a model of this kind, which only takes into account the relative energies of the transition states through which the various isomeric intermediates are transformed into their corresponding products, to calculate the product distribution, requires that the Curtin–Hammet principle be applicable, that is, that the interconversion of the said intermediates be faster than their evolution into the corresponding products. However, the VT-NMR studies, in combination with X-ray analysis of [Ir(cod)(**L1 d**)][BAr_F], suggest that, at least at the level of the Ir^{I} catalyst precursors, the *R* configuration is maintained at the sulfur center in solution. To address these concerns, the transition states for the interconversion of the intermediates **A7** and **A8** were calculated. The results clearly show that the barrier for pyramidal inversion at the sulfur center is considerably lower than the barriers leading to product formation, thus confirming the applicability of the Curtin–Hammet principle and the validity of the theoretical model (Table SI.3 in the Supporting Information).

Figure 3 shows the most stable calculated transition states (TS) for the major and the minor pathway with both ligands. In these key transition states we can see, on the one hand, the proximity of the phenyl moiety in the ligand backbone group to the thioether substituent and, on the other hand, that the hydrogen at the *ortho* position of the phenyl group in the ligand skeleton is pointing towards the metal center. All these findings indicate that the aromatic substituent in the ligand backbone could have an important influence on the enantioselectivity.

These features prompted us to recalculate the relevant transition states (from **A1** for the major pathway and **A8** for the minor pathway) by replacing the phenyl group by a mesityl group (ligand **L10 d**; Figure 1). The results, which are summarized in Table 3, showed that the energy difference between the two transition states was unrealistically large (30.9 kJ mol^{-1}). In Figure 4, it can be seen that in the transition state giving the *S* product there is a great steric interaction between the thioether substituent and the mesityl group, essen-

Table 2. Calculated energies for the transition states TS_{MI} and TS_{META} with substrate **S1** using ligands **L1d** and **L6d**.[a]

Starting geometry	TS_{MI} L1d	TS_{MI} L6d	Starting geometry	TS_{META} L1d	TS_{META} L6d
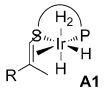 **A1** *si* face coordination *R* config. on sulfur	0	0	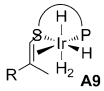 **A9** *si* face coordination *R* config. on sulfur	17.0	20.2
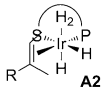 **A2** *si* face coordination *S* config. on sulfur	20.0	30.5	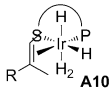 **A10** *si* face coordination *S* config. on sulfur	20.2	26.0
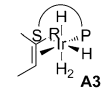 **A3** *si* face coordination *R* config. on sulfur	25.5	36.7	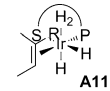 **A11** *si* face coordination *R* config. on sulfur	31.8	34.3
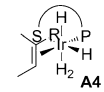 **A4** *si* face coordination *S* config. on sulfur	19.1	30.3	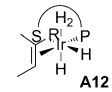 **A12** *si* face coordination *S* config. on sulfur	32.7	44.1
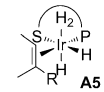 **A5** *re* face coordination *R* config. on sulfur	9.8	19.0	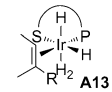 **A13** *re* face coordination *R* config. on sulfur	31.7	36.3
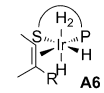 **A6** *re* face coordination *S* config. on sulfur	22.6	35.1	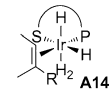 **A14** *re* face coordination *S* config. on sulfur	34.6	42.9
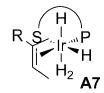 **A7** *re* face coordination *R* config. on sulfur	18.2	20.5	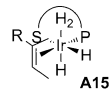 **A15** *re* face coordination *R* config. on sulfur	13.1	21.1
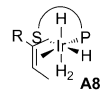 **A8** *re* face coordination *S* config. on sulfur	4.5	8.5	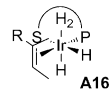 **A16** *re* face coordination *S* config. on sulfur	26.2	31.0

[a] Energies in kJ mol^{-1}; R = 4-MeO-C_6H_4.

tially locking the configuration at the sulfur center to *R*. We therefore switched from an *S* configuration at the sulfur center to an *R* configuration choosing again the most stable isomers previously calculated for ligands **L1d** and **L6d** (TS from **A5**, **A7**, and **A15**; Table 3). Thus, the obtained energy difference between the two most stable transition states responsible for the formation of both enantiomers of the hydrogenated product was 14.2 kJ mol^{-1} (ligand **L10d**) surpassing the $\Delta\Delta G^{+}_{calcd}$ with ligands **L1d** and **L6d** (4.5 kJ mol^{-1} and 8.5 kJ mol^{-1}, respectively), indicating that this new modification should provide higher enantioselectivities than the Ir-**L1d** and Ir-**L6d** catalysts.

Encouraged by this result and having in mind that the catalytic experiments using phenyl glycidol-based ligands (**L1**–**L9**) showed that replacing the diphenyl phosphinite moiety by *o*-tolyl groups has a positive effect on enantioselectivity (i.e., Table 1, entries 27 and 28), we also performed the calculations of the relevant transition states with the mesityl-based ligand **L10e** (Figure 1), with tolyl groups at the phosphinite moiety. However, the calculated energy difference between the most stable transition states thus obtained was 13.7 kJ mol^{-1}, very similar to that achieved with ligand **L10d** (Table 3 and Figure 5). So, in contrast to that observed for ligands **L1**–**L9**, containing a phenyl group in the backbone (see above), the steric bulk of the phosphinite group should have little impact on enantioselectivity for the mesityl-based ligands.

With these latter theoretical results in hand, a decision was made to prepare and screen thioether-phosphinite ligands **L10d** and **L10e**, with a mesityl group, in the asymmetric hydrogenation of substrate **S1**. The experimental results are shown in Table 4 (entries 3 and 4). As predicted by the theoretical calculations, both mesityl-based ligands afforded similar higher enantioselectivities than ligands **L1**–**L9**. If we compare the calculated and experimental values (Table 4), we can conclude that, despite the fact that the calculated free-energy differences are systematically higher than the experimental values, the general trend is reproduced well. The robustness of the theoretical model is demonstrated with the prediction of the new improved ligands **L10d** and **L10e** containing a mesityl group.

Asymmetric hydrogenation of other minimally functionalized olefins: Scope and limitations

To establish the scope of the new family of ligands in the Ir-catalyzed hydrogenation, we selected a representative family of substrates. We first studied the asymmetric hydrogenation of other *E*- and *Z*-trisubstituted olefins (**S2**–**S18**), including examples containing neighboring polar groups, by using the P,S-ligand library **L1**–**L10a**–**g**. The most noteworthy results are shown in Table 5 (see the Supporting Information for a complete set of results). We found again that the correct choice of the ligand parameters is crucial to achieve the highest levels of

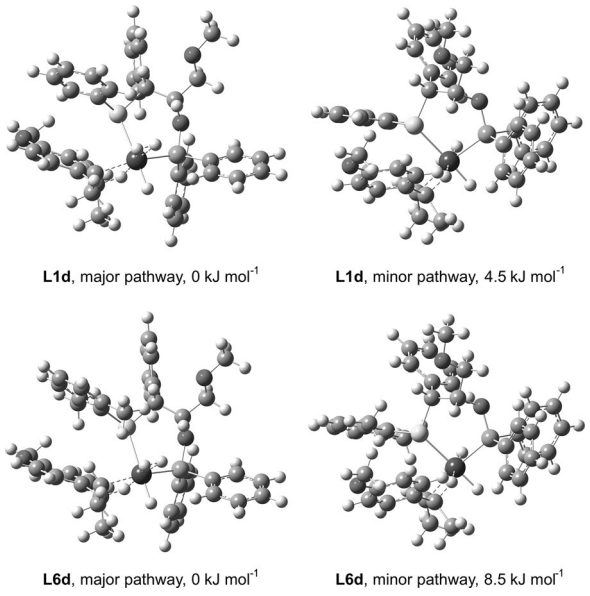

Figure 3. Calculated transition states (TS) for the major and the minor pathways with ligands **L1d** and **L6d**.

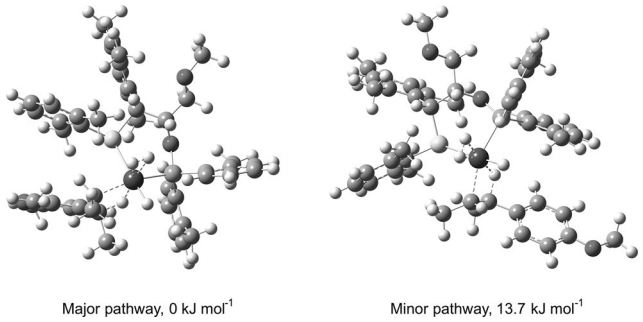

Figure 5. Calculated transition states (TS) for the major and the minor pathways with ligand **L10e**.

to >99%; Table 5, entries 2, 3, 5, and 6). The result followed the same trends as those observed for substrate **S1**. Enantioselectivities were thus best with the optimized ligands **L10d** and **L10e**.

To assess the potential of the new ligand library for *Z*-trisubstituted isomers, which are usually hydrogenated less enantioselectively than the corresponding *E*-isomers, we chose substrates **S4** and **S5** (Table 5, entries 7–12). The reduction of the model *Z* substrate **S4** proceeded with moderate enantiocontrol and followed a different trend than that observed with *E* substrates **S1**–**S3**. The enantioselectivities were thus best with ligands **L6a** and **L6c** (Table 5, entries 7 and 8). The moderate enantioselectivity can be explained by a competition between direct hydrogenation versus *Z*/*E*-isomerization of the substrate. The hydrogenation of the *E* isomer produces the opposite configuration of the hydrogenated product than when the *Z* isomer is hydrogenated, which results in low enantioselectivity.[2d] Accordingly, the reduction of dehydronaphthalene **S5**, which has a *Z* configuration and for which *Z*/*E*-isomerization is not possible, produces higher

Table 3. Calculated energies for the relevant transition states with substrate **S1** using ligands **L10d** and **L10e**.[a]

Starting geometry	L10d	L10e	Starting geometry	L10d	L10e
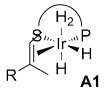 **A1** *si* face coordination *R* config. on sulfur	0	0	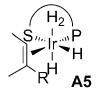 **A5** *re* face coordination *R* config. on sulfur	14.2	13.7
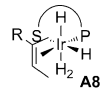 **A8** *re* face coordination *S* config. on sulfur	30.9	36.7	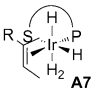 **A7** *re* face coordination *R* config. on sulfur	28.4	33.2
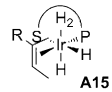 **A15** *re* face coordination *R* config. on sulfur	19.9	37.5			

[a] Energies in kJ mol^{-1}; R = 4-MeO-C_6H_4.

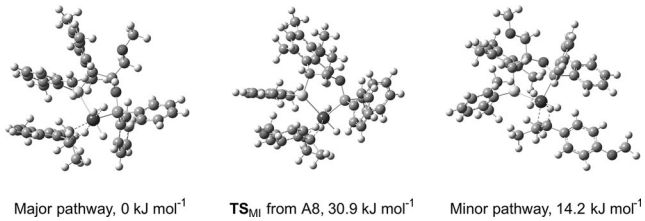

Figure 4. Calculated transition states (TS) for the major and the minor pathways with ligand **L10d**.

enantioselectivity. We initially studied the hydrogenation of *E* substrates **S2** and **S3**, related to **S1**, which differ in the substituents of both the aryl ring and the substituents *trans* to the aryl group. Excellent enantioselectivities, even higher than with the model substrate **S1**, were obtained (*ee* values between 98

Table 4. Comparison between experimental and theoretical results.[a]

Entry	Ligand	*ee*[a] [%]	$\Delta\Delta G^{+}_{exptl}$[b]	$\Delta\Delta G^{+}_{calcd}$[b]
1	**L1d**	44 (*R*)	2.3	4.5
2	**L6d**	64 (*R*)	3.8	8.5
3	**L10d**	94 (*R*)	8.6	14.2
4	**L10e**	95 (*R*)	9.1	13.7

[a] Reaction conditions: 0.5 mmol of **S1**, 2 mol% catalyst precursor, CH_2Cl_2 as solvent, 100 bar H_2, 4 h. Full conversions were achieved in all cases. The *ee* values were measured by GC. [b] Energies in kJ mol^{-1}.

Table 5. Selected results for the Ir-catalyzed hydrogenation of **S2**–**S18** using the P,S-ligand library **L1**–**L10a**–**g**.[a]

Entry	Substrate	Product	L	*ee*[b] [%]	Entry	Substrate	Product	L	*ee*[b] [%]
1	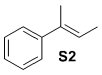 **S2**	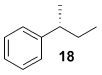 **18**	**L8e**	99 (*R*)	28	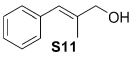 **S11**	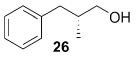 **26**	**L7e**	78 (*R*)
2			**L10d**	99 (*R*)	29			**L8e**	79 (*R*)
3			**L10e**	>99 (*R*)	30			**L10e**	81 (*R*)
4	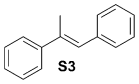 **S3**	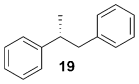 **19**	**L8e**	97 (*R*)	31	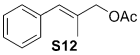 **S12**	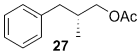 **27**	**L7e**	81 (*R*)
5			**L10d**	98 (*R*)	32			**L8e**	80 (*R*)
6			**L10e**	99 (*R*)	33			**L10e**	85 (*R*)
7	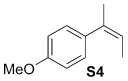 **S4**	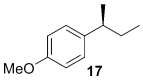 **17**	**L6a**	62 (*S*)	34	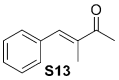 **S13**	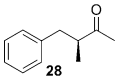 **28**	**L6d**	94 (*S*)
8			**L6c**	62 (*S*)	35			**L10d**	98 (*S*)
9			**L10e**	58 (*S*)	36			**L10e**	99 (*S*)
10	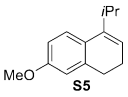 **S5**	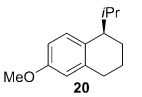 **20**	**L8c**	36 (*R*)	37	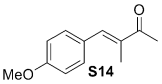 **S14**	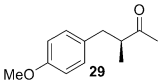 **29**	**L6d**	96 (*S*)
22			**L8e**	78 (*R*)	38			**L10d**	97 (*S*)
12			**L10e**	82 (*R*)	39			**L10e**	99 (*S*)
13	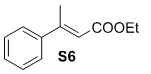 **S6**	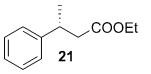 **21**	**L8e**	>99 (*R*)	40	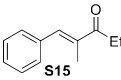 **S15**	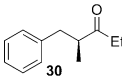 **30**	**L6d**	95 (*S*)
14			**L10d**	99 (*R*)	41			**L10d**	98 (*S*)
15			**L10e**	>99 (*R*)	42			**L10e**	98 (*S*)
16	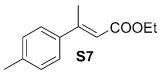 **S7**	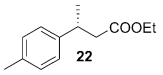 **22**	**L8e**	99 (*R*)	43	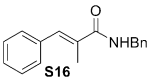 **S16**	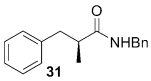 **31**	**L8e**	70 (*S*)
17			**L10d**	99 (*R*)	44			**L10d**	69 (*S*)
18			**L10e**	99 (*R*)	45			**L10e**	72 (*S*)
19	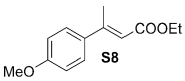 **S8**	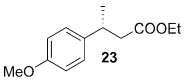 **23**	**L8e**	98 (*R*)	16	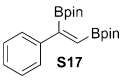 **S17**	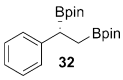 **32**	**L9d**	43 (*R*)
20			**L10d**	98 (*R*)	47			**L10d**	44 (*R*)
21			**L10e**	99 (*R*)	48			**L10e**	45 (*R*)
22	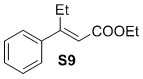 **S9**	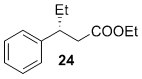 **24**	**L8e**	99 (*R*)	49	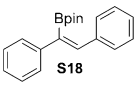 **S18**	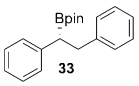 **33**	**L7a**	94 (+)
23			**L10d**	99 (*R*)	50			**L7c**	93 (+)
24			**L10e**	99 (*R*)	51			**L10e**	83 (+)
25	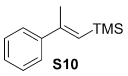 **S10**	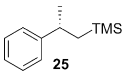 **25**	**L7e**	60 (*R*)					
26			**L8e**	61 (*R*)					
27			**L10e**	68 (*R*)					

[a] Reactions carried out using 0.5 mmol of substrate, 2 mol% of Ir-catalyst precursor, CH_2Cl_2 as solvent, 100 bar H_2, 4 h. Full conversions were achieved in all cases. [b] Enantiomeric excesses determined by chiral GC or HPLC.

enantioselectivities (*ee* values up to 82%; Table 5, entry 12). Moreover in contrast to **S4**, the best enantioselectivities were achieved with the optimized mesityl-based ligands **L10d** and **L10e**.

We next studied the reduction of a wide range of trisubstituted olefins containing several types of neighboring polar groups **S6**–**S18** (Table 5, entries 13–51). The hydrogenation of this type of substrate is especially relevant because they allow for further functionalization and could therefore be important intermediates for the synthesis of more complex chiral molecules. We were pleased to find that enantioselectivities are among the best observed in most of the examples. A range of α,β-unsaturated esters (**S6**–**S9**) were thus efficiently hydrogenated (*ee* values ranging from 98% to >99%). It should be noted that the *ee* values are highly independent of the nature of the alkyl substituent and the electronic nature of the substrate phenyl ring. Although enantioselectivities follow the same trend regarding the effect of the thioether, alkoxy, and the P-donor group, the nature of the aryl group in the ligand backbone is less pronounced. Enantioselectivities were thus best with ligands **L6e**, **L8e**, **L10d**, and **L10e**. On the other hand, the presence of a trimethylsilyl group in the substrate (**S10**) has a negative effect on enantioselectivity (Table 5, entries 25–27), whereas the reduction of allylic alcohol and acetate **S11** and **S12** provided higher enantioselectivities (*ee* values up to 85%, Table 5, entry 33). The use of the optimized mesityl-based ligands **L10d** and **L10e** was essential to achieve the highest levels of enantioselectivity in the reduction of several α,β-unsaturated ketones **S13**–**S15** (*ee* values ranging from 98 to 99%; Table 5, entries 34–42), for which the previous furanoside P–S ligands proved to be unsuccessful.[27] This represents an important entry point to the formation of ketones with stereogenic centers in the α position to the carbonyl group. Despite this, they have been less studied than other trisubstituted olefins with a neighboring polar group.[2d] Other challenging substrate types that have been less investigated are the α,β-unsaturated amides (**S16**)[28] and alkenylboronic esters (**S17** and **S18**).[29] Amides with stereogenic centers in the α position are an important class of compounds since this motif is present in several natural products and they can be easily transformed into other useful compounds (i.e., amines).[30] The hydrogenation of alkenylboronic esters provides easy access to chiral borane compounds, which are valuable organic intermediates since the C–B bond can be easily transformed to C–O, C–N and C–C bonds with retention of the chirality.[31] The hydrogenation of α,β-unsaturated amide **S16** followed the same trend as substrate **S1**. Enantioselectivities up to 72% were thus achieved with ligand **L10e**. The reduction of alkenylboronic esters followed a different trend than **S1**. Whereas for the more studied substrate **S17** moderate

enantioselectivities were achieved, for the less studied substrate **S18** high enantioselectivities up to 94% were reached using phosphite-thioether ligands **L7a** and **L7c**. These results again showed the importance of having a modular ligand design.

The stereochemical outcome in the reduction of these trisubstituted olefins can be easily rationalized by using a quadrant diagram based on the optimized DFT calculated structures of the transition states (Figure 6). In this quadrant model we found that the thioether substituent blocks the upper-left quadrant and one of the P-aryl groups partly occupies the lower-right quadrant making it semi-hindered. The other two quadrants, which are free from bulky groups, are open. The DFT structures thus show that the Ir–PS catalysts generate a pocket that is well suited to olefins with large *trans* substituents (*E*-olefins; Figure 6a). This fully explains the high enantioselectivities obtained with the DFT-optimized thioether-phosphinite ligands in the reductions of olefins **S1**–**S3**, **S6**–**S9**, **S11**, and **S12**. However, the reduction of substrates **S13**–**S16** gives products with the opposite absolute configuration to what is suggested by the quadrant model as previously observed for α-substituted-α,β-unsaturated esters.[2d,32] On the other hand, in the reduction of alkenylboronic ester **S18**, the bulky pinacolato boron group (Bpin) faces the steric bulk of the ligand in the semi-hindered lower-right quadrant. Thus the need to switch to phosphite ligands **L7a** and **L7c** to obtain high enantioselectivity could be justified by the flexibility of the biphenyl phosphite moiety,[33] which could tune the steric hindrance of this lower-right quadrant so that it can accommodate the pinacolato boron substituent of the substrate.

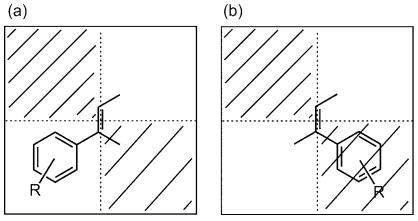

Figure 6. Quadrant diagram describing the substrate–ligand interactions.

By using this quadrant model, we can also explain the change in the sense of enantioselectivity observed experimentally when using *Z*-trisubstituted olefins instead to *E*-olefins. The Z-olefin must coordinate preferentially through the *re* face, with the aryl substituent in the semi-hindered lower-right quadrant and the hydrogen atom positioned in the hindered upper-left quadrant (Figure 6b). This model also explains the lower enantioselectivities when the optimized ligands were used in the reduction of *Z*-olefins. The favorable chiral pocket for *E*-olefins generated by our Ir–PS catalysts, which can accommodate large *trans* substituents, fails to perfectly control the face coordination preference of the *Z*-olefins.

To assess the potential of the ligand library **L1**–**L10a**–**g** for the more challenging 1,1-disubstitued olefins, which generally are hydrogenated less enantioselectively than the corresponding trisubstituted ones, we next chose to hydrogenate substrate **S19** as a model. The lower enantioselectivity obtained with 1,1-disubstituted terminal olefins than that obtained with trisubstituted olefins has been attributed to two main motives.[2d,7a,e] The first is that enantiofacial olefin coordination is difficult to control due to the comparable steric size of the alkyl and aryl substituent at the olefinic C atom. The second reason is that the terminal double bond can undergo isomerization under hydrogenation conditions to produce the more stable internal *trans*-alkene, whose hydrogenation leads to the predominant formation of the opposite enantiomer of the product. The results under optimized conditions are shown in Table 6.

Table 6. Ir-catalyzed hydrogenation of **S19** using the P,S-ligand library **L1**-**L10a**–**g**.[a]

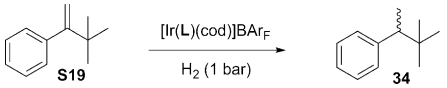

Entry	Ligand	*ee*[b] [%]	Entry	Ligand	*ee*[b] [%]
1	**L1a**	46 (*S*)	20	**L6b**	95 (*S*)
2	**L1b**	70 (*S*)	21	**L6c**	94 (*R*)
3	**L1c**	82 (*R*)	22	**L6d**	93 (*S*)
4	**L1d**	64 (*S*)	23	**L6e**	96 (*S*)
5	**L2b**	88 (*S*)	24	**L7a**	30 (*S*)
6	**L2c**	74 (*R*)	25	**L7b**	78 (*S*)
7	**L2e**	81 (*S*)	26	**L7c**	82 (*R*)
8	**L3a**	31 (*S*)	27	**L7d**	76 (*S*)
9	**L3b**	93 (*S*)	28	**L7e**	72 (*S*)
10	**L3c**	93 (*R*)	29	**L7f**	54 (*S*)
11	**L3e**	75 (*S*)	30	**L8a**	66 (*S*)
12	**L4a**	62 (*S*)	31	**L8e**	90 (*S*)
13	**L4b**	60 (*S*)	32	**L9a**	30 (*S*)
14	**L4c**	92 (*S*)	33	**L9b**	64 (*S*)
15	**L4d**	87 (*S*)	34	**L9c**	76 (*R*)
16	**L4e**	80 (*S*)	35	**L9d**	69 (*S*)
17	**L5a**	64 (*S*)	36	**L10d**	97 (*S*)
18	**L5e**	76 (*S*)	37	**L10e**	97 (*S*)
19	**L6a**	94 (*S*)	38[c]	**L10e**	97 (*S*)

[a] Reactions carried out using 0.5 mmol of **S19**, 2 mol% of Ir-catalyst precursor, CH_2Cl_2 as solvent, 1 bar H_2, 4 h. Full conversions were achieved in all cases except for entries 9 and 10 (86 and 96% conversion, respectively). [b] The *ee* values were determined by chiral GC. [c] Reaction carried out using 0.25 mol% of Ir-catalyst precursor for 8 h.

We were again able to fine-tune the ligand parameters to achieve high activities and enantioselectivities (*ee* values up to 97%) in the reduction of this substrate at low catalyst loadings (0.25 mol%) and hydrogen pressures (1 bar).

The results showed that the effect on enantioselectivity of the thioether and the alkoxy substituents and the aryl-glycidol group follow the same trend as for **S1**. However, in contrast to **S1**, enantioselectivities for substrate **S19** are similar for ligands containing either an enantiopure biaryl phosphite moiety (**b**,**c**) or a diaryl phosphinite group (**d**,**e**; i.e., Table 6, entries 20–23). Interestingly, we found that the sense of enantioselectivity is controlled by the configuration of the biaryl phosphite group (Table 6, entries 20 and 21), and this represents an additional

possibility for the control of the absolute configuration of the products through ligand modification.[34] As observed for **S1**, the tropoisomerism in the fluxional biaryl phosphite group **a** is not controlled by the ligand backbone, except for ligand backbone **L6**, containing an 2,6-dimethylphenyl thioether substituent, which provided similar high enantioselectivities as the enantiopure phosphite counterparts (Table 6, entries 19 vs. 20 and 21).

We then investigated the scope of the new ligand library in the asymmetric hydrogenation of other 1,1-disubstituted substrates (Table 7). The results with substrates **S19**–**S21** indicated that enantioselectivity is affected by the alkyl chain substituent (*ee* values ranging from 27 to 97%; Table 6, entries 36 and 37; and Table 7, entries 3 and 6). This can be explained by the competition between isomerization versus direct hydrogenation for substrates **S20** and **S21**. Accordingly, high amounts of isomerized internal olefins were observed as byproducts in the hydrogenation of **S20** and **S21**.

We next turned our attention to study substrates with neighboring polar groups (**S22**–**S29**), due to their importance in the preparation of chiral synthons. The reduction of substrates **S22** and **S23**, containing trimethylsilyl and acetate groups, respectively, provided moderate enantioselectivities (up to 71%; Table 7, entries 7–12). To study whether these enantioselectivities could be due again to their isomerization to the trisubstituted internal olefins under the reaction conditions, a decision was made to hydrogenate olefins containing trifluoromethyl and boronate neighboring groups, which cannot undergo isomerization (substrates **S24** and **S25**). The hydrogenation of substrate **S24** proceeded with excellent enantiocontrol (*ee* values up to 99%; Table 7, entries 13–15).[35] These results are of interest because enantioenriched α-trifluoromethyl chiral molecules are relevant building blocks for the development of agrochemicals, pharmaceuticals, and materials owing to the unique properties of the fluorine atom.[36] Interestingly, the reduction of alkenylboronic ester **S25** also provided high enantioselectivities (up to 91%, Table 7, entry 18). Encouraged by this latter result we also tested other challenging terminal boronic esters **S26**–**S29** (Table 7, entries 19–30). Although these substrates are also prone to isomerization they can be reduced with acceptable values of enantioselectivity (up to 84%). If we compare these latter results with those achieved by the only successful report on this substrate class using Ir-phosphinite-imidazoline ligands,[29b] we can conclude that the new P,S catalytic systems overcome the limitation of the Pfaltz ligands in the hydrogenation of **S25** and **S29**, for which poor enantioselectivities were reported (*ee* values up to 4% for **S25** and 33% for **S29** at −20 °C).[29b]

Finally, we could also obtain excellent enantioselectivity in the hydrogenation of heteroaromatic alkene **S30** (*ee* values up to 96%, Table 7, entry 33). Substrates containing heteroaraomatic groups are popular in fine-chemistry industries since the heterocyclic part allows for further functionalization.

Table 7. Selected results for the Ir-catalyzed hydrogenation of **S20**–**S30** using the P,S-ligand library **L1**–**L10a**–**g**.[a]

Entry	Substrate	Product	L	*ee*[b] [%]
1	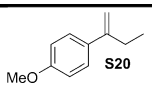 **S20**	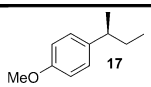 **17**	**L6a**	34 (*S*)[c]
2			**L6e**	54 (*S*)[d]
3			**L10e**	62 (*S*)[e]
4	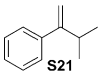 **S21**	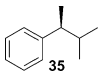 **35**	**L6a**	16 (*S*)[f]
5			**L6e**	21 (*S*)[g]
6			**L10e**	27 (*S*)[h]
7	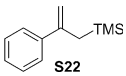 **S22**	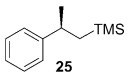 **25**	**L7a**	29 (*R*)
8			**L7c**	58 (*R*)
9			**L10e**	71 (*R*)
10	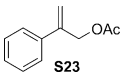 **S23**	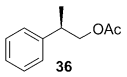 **36**	**L7a**	43 (*R*)
11			**L7c**	52 (*R*)
12			**L10e**	68 (*R*)
13	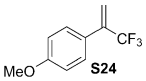 **S24**	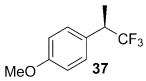 **37**	**L1a**	99 (−)
14			**L1c**	99 (−)
15			**L8e**	99 (−)
16	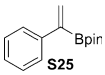 **S25**	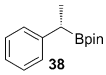 **38**	**L3c**	74 (*S*)
17			**L10d**	55 (*S*)
18			**L3c**	91 (*S*)[i]
19	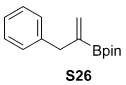 **S26**	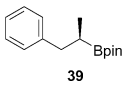 **39**	**L1c**	72 (*R*)
20			**L3c**	74 (*R*)
21			**L10d**	28 (*R*)
22	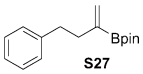 **S27**	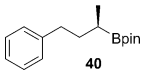 **40**	**L1c**	76 (*R*)
23			**L3c**	81 (*R*)
24			**L10d**	19 (*R*)
25	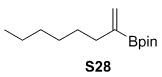 **S28**	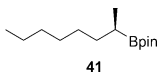 **41**	**L1c**	76 (*R*)
26			**L6c**	77 (*R*)
27			**L10e**	62 (*R*)
28	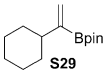 **S29**	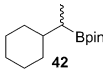 **42**	**L1c**	76 (*S*)
29			**L10d**	75 (*R*)
30			**L10e**	84 (*R*)
31	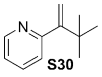 **S30**	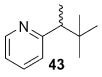 **43**	**L6b**	95 (+)
32			**L6c**	94 (−)
33			**L10e**	96 (+)

[a] Reactions carried out using 0.5 mmol of substrate, 2 mol% of Ir-catalyst precursor, CH_2Cl_2 as solvent, 1 bar H_2, 4 h. Full conversions were achieved in all cases. [b] The *ee* values were determined by chiral GC or HPLC. [c] 38% of isomerized **S1** and 2% of **S2**. [d] 32% of isomerized **S1**. [e] 35% of isomerized **S1**. [f] 41% of tetrasubstituted olefin. [g] 32% of tetrasubstituted olefin. [h] 29% of tetrasubstituted olefin. [i] Reaction carried out at −20 °C.

Asymmetric hydrogenation using propylene carbonate as environmentally benign solvent: Recycling experiments

Finally, we focused our attention to replace the widely used dichloromethane solvent with propylene carbonate (PC) as an environmentally benign solvent.[37] The use of PC as solvent not only allows the hydrogenation to be performed in a more sustainable way but also makes possible the recycling of the Ir catalysts by a simple two-phase extraction.[38] Catalyst recycling is desirable in large-scale processes due to the high cost of iridium.

To assess whether the new Ir–P,S catalysts could be employed by using PC as solvent, we screened the Ir-**L10e** catalytic system in the hydrogenation of model substrates **S1** and **S19** (Table 8). Although the reaction rates are lower in PC than in dichloromethane, similar high enantioselectivities were achieved (*ee* values up to 94% for **S1** and 96% for **S19**). In addition, we were able to recycle the Ir catalysts up to 3 times without any drop of enantioselectivity. As previously observed, the reaction times necessary to achieve high conversions increased.[38] This drop in activity could be attributed to the loss of iridium catalyst to the hexane phase,[10k,38a] to the formation of inactive iridium clusters,[39] or to both.

Table 8. Asymmetric hydrogenation using propylene carbonate using catalyst precursor [Ir(cod)(**L10e**)][BAr_F]. Recycling experiments.[a]

Cycle	Substrate	% Conv.[b] (*t* [h])	*ee*[c] [%]
1[d]	**S1**	98 (6)	94 (*R*)
2[d]		84 (10)	94 (*R*)
3[d]		89 (15)	93 (*R*)
1[e]	**S19**	97 (4)	95 (*S*)
2[e]		96 (8)	96 (*S*)
3[e]		81 (10)	95 (*S*)
1[e]	**S20**	99 (6)[f]	72 (*S*)

[a] Reactions carried out using 0.5 mmol of substrate and 2 mol% of Ir-catalyst precursor. [b] Conversion measured from the ^{1}H NMR spectrum for substrate **S1** or by GC for substrates **S19** and **S20**. [c] The *ee* values were determined by chiral HPLC (substrate **S1**) or GC (substrates **S19** and **S20**). [d] Reaction carried out at 125 bar. [e] Reaction carried out at 50 bar. [f] 18% of **S1** observed.

Another important feature of using PC as a solvent in the asymmetric hydrogenation using Ir-P/N catalytic systems, observed by Börner et al., is that the rate of isomerization of terminal olefins to the corresponding trisubstituted ones diminishes compared with when dichloromethane is used. This behavior was exploited to improve enantioselectivity in the reduction of 1-methylene-1,2,3,4-tetrahydronaphthalene, which easily isomerizes to form the trisubstituted olefin.[10k,38a] We therefore also performed the asymmetric hydrogenation of substrate **S20** with Ir-**L10e** using PC as solvent. We were pleased to find that the amount of isomerized trisubstituted substrate substantially diminished, and that the enantioselectivity consequently improved (*ee* values up to 72%, compared with 62% in dichloromethane).

Conclusion

A modular ligand design, with the help of DFT studies, has been shown to be highly successful in the identification and tuning of the crucial stereodefining groups to generate more selective catalysts. Following this approach, a library of modularly constructed thioether-phosphinite/phosphite ligands derived from the ring opening of enantiopure epoxides has been evaluated in the asymmetric iridium-catalyzed hydrogenation of a wide range of olefins. An extensive study on the influence of the different structural parameters has been performed, demonstrating the highly modular nature of these ligands. Computations gave an understanding of the enantiocontrol in the reaction allowing rationalization of the modifications required for improving selectivity. The computations moreover indicated that the diastereoisomers resulting from coordination of the thioether to the metal center interconvert rapidly under the reaction conditions through pyramidal inversion, thus allowing for the use of the Curtin–Hammet principle in predicting the outcome of the reaction. In general, enantioselectivities are mainly controlled by the nature of the thioether, the aryl moieties and the type of P-donor group. However, the effect of changing these modules depends on the substrate class. The degree of activity and stereoinduction achieved with the lead ligands were amongst the highest with respect to the ones reported in the literature. The asymmetric hydrogenations were also performed using propylene carbonate as solvent, which allowed the Ir catalyst to be reused.

Experimental Section

General considerations

All reactions were carried out by using standard Schlenk techniques under an argon atmosphere. Solvents were purified and dried by standard procedures. Phosphorochloridites were easily prepared in one step from the corresponding biphenols.[40] Intermediate compounds **1**--**2**,[18] **3**--**8**,[17] **10**--**13**,[17] and **15**;[17] and thioether-phosphinite ligands **L1d**,[17] **L4d**,[17] **L6L7d**,[17] and **L9d**[17] were prepared as previously reported. ^{1}H, ^{13}C, and ^{31}P NMR spectra were recorded using a 400 MHz spectrometer. Chemical shifts are relative to that of $SiMe_4$ (^{1}H and ^{13}C) as internal standard or H_3PO_4 (^{31}P) as external standard. ^{1}H, ^{13}C and ^{31}P assignments were made on the basis of ^{1}H-^{1}H gCOSY, ^{1}H-^{13}C gHSQC and ^{1}H-^{31}P gHMBC experiments.

Computational details

Geometries of all transition states were optimized using the Gaussian 09 program,[23] employing the B3LYP[20] density functional and the LANL2DZ[21d] basis set for iridium and the 6–31G*[21a–c] basis set for all other elements. Solvation correction was applied in the course of the optimizations using the PCM model with the default parameters for dichloromethane.[22] The complexes were treated with charge +1 and in the singlet state. No symmetry constraints were applied. Normal mode analysis of all transition states revealed a single imaginary mode corresponding to the expected hydride transfer or σ-bond metathesis. In the case of hydride transfer, concomitant cleavage of the dihydrogen ligand was observed. The energies were further refined by performing single point calculations

using the abovementioned parameters, with the exception that the 6–311+G**[24] basis set was used for all elements except iridium, and by applying dispersion correction using the DFT-D3[25] model. All energies reported are Gibbs free energies at 298.15 K and calculated as $G_{reported} = G_{6\text{-}31G^*} + E_{6\text{-}311+G^{**}} - E_{6\text{-}31G^*} + E_{DFT\text{-}D3}$

General procedure for the preparation of thioether-alcohols 9, 14, and 16

To a suspension of the desired chiral epoxide (1.34 mmol) and sodium hydroxide (107 mg, 2.68 mmol, 2 equiv) in dioxane/water (10:1 v/v, 6.6 mL) was added the corresponding thiol (2.68 mmol, 2 equiv). The mixture was heated for 4 h at 90 °C. The reaction was monitored by TLC until disappearance of the starting epoxide. The mixture was left to reach RT and then water (15 mL) was added. The mixture was extracted with CH_2Cl_2 (3×15 mL). The combined organic extracts were washed with brine, dried with Na_2SO_4, and filtered. The solvent was removed under vacuum and the crude was purified by flash chromatography on SiO_2 to produce the desired thioether-alcohol as a white solid.

General procedure for the preparation of the thioether-phosphite ligands L1–L9 a–c

The corresponding phosphorochloridite (0.55 mmol) produced in situ was dissolved in toluene (2.5 mL), and pyridine (0.15 mL, 2.9 mmol) was added. The corresponding thioether-hydroxyl compound (0.5 mmol) was azeotropically dried with toluene (3×2 mL) and then dissolved in toluene (2.5 mL) to which pyridine (0.15 mL, 2.9 mmol) was added. The alcohol solution was then transferred slowly to the phosphorochloridite solution. The reaction mixture was stirred at 80 °C for 90 min, after which the pyridine salts were removed by filtration. Evaporation of the solvent gave a white foam, which was purified by flash chromatography on alumina (toluene/NEt_3 = 100:1) to produce the corresponding ligand as a white solid.

General procedure for the preparation of the thioether-phosphinite ligands L1–L10 d–g

The corresponding thioether-hydroxyl compound (0.5 mmol) and 4-dimethylaminopyridine (DMAP; 6.7 mg, 0.055 mmol) were dissolved in toluene (1 mL), and triethylamine was added (0.09 mL, 0.65 mmol) at RT, followed by the addition of the corresponding chlorophosphine (0.55 mmol) through a syringe. The reaction was stirred for 20 min at RT. The solvent was removed in vacuo, and the product was purified by flash chromatography on alumina (toluene/NEt_3 = 100:1) to produce the corresponding ligand as an oil.

General procedure for the preparation of [Ir(cod)(L)][BAr_F] (L = L1–L10 a–g)

The corresponding ligand (0.074 mmol) was dissolved in CH_2Cl_2 (5 mL) and [Ir(μ-Cl)(cod)]$_2$ (25.0 mg, 0.037 mmol) was added. The reaction mixture was heated at reflux at 50 °C for 1 hour. After 5 min at room temperature, NaBArF (77.2 mg, 0.080 mmol) and water (5 mL) were added and the reaction mixture was stirred vigorously for 30 min at room temperature. The phases were separated and the aqueous phase was extracted twice with CH_2Cl_2. The combined organic phases were dried with $MgSO_4$, filtered through a plug of Celite and the solvent was evaporated to give the product as a red-orange solid.

Typical procedure for the hydrogenation of olefins

The alkene (0.5 mmol) and Ir complex (2 mol%) were dissolved in CH_2Cl_2 (2 mL) in a high-pressure autoclave, which was purged four times with hydrogen. Then, it was pressurized at the desired pressure. After the desired reaction time, the autoclave was depressurized and the solvent evaporated off. The residue was dissolved in Et_2O (1.5 mL) and filtered through a short Celite plug. The enantiomeric excess was determined by chiral GC or chiral HPLC and conversions were determined by ^{1}H NMR spectroscopy. The enantiomeric excesses of hydrogenated products from **S1**,[14a] **S2**,[41] **S3** and **S4**,[14a] **S5**,[42] **S6**,[14a] **S7**–**S9**,[10m] **S10**,[43] **S11** and **S12**,[14a] **S13**–**S15**,[10j] **S16**,[28] **S17**,[29a] **S18**,[29b] **S19**,[14a] **S20**,[10 g] **S21**,[14a] **S22**,[43] **S23**,[44] **S24**,[10k] **S25**–**S29**,[29b] and **S30**[14a] were determined by using the conditions previously described.

Typical procedure for reutilization of catalysts by using PC as a solvent

After each catalytic experiment, the autoclave was depressurized. We then extracted the colorless propylene carbonate solution with dry/deoxygenated hexane under argon atmosphere with the aim to remove the remaining substrate and the hydrogenated olefin. After the extractions, the corresponding amount of substrate (0.5 mmol) was then added and a new catalytic experiment was started.

Acknowledgements

X.C., E.K., and M.A.P. thank MINECO (grants CTQ2008-00947/BQU and CTQ2012-38594-C02-01), Generalitat de Catalunya (grant 2009SGR623), EU-ITN network Mag(net)icFun (PITN-GA-2012-290248), and the ICIQ Foundation for financial support. J.M., M.C., J.M., O.P., and M.D. thank the Spanish Government for providing grant CTQ2010-15835, the Catalan Government for grant 2009SGR116, and the ICREA Foundation for providing M.D. and O.P. with financial support through the ICREA Academia awards.

Keywords: asymmetric synthesis · density functional theory · hydrogenation · iridium · ligands

[1] a) R. Noyori, *Asymmetric Catalysis in Organic Synthesis*, Wiley, New York, **1994**; b) E. N. Jacobsen, A. Pfaltz, H. Yamamoto, *Comprehensive Asymmetric Catalysis, Vol. 1*, Springer, Berlin, **1999**; c) I. Ojima, *Catalytic Asymmetric Synthesis*, 2ednd edWiley-VCH, Weinheim, **2000**; d) H.-U. Blaser, E. Schmidt, *Asymmetric Catalysis on Industrial Scale*, Wiley, New York, **2004**; e) C. A. Busacca, D. R. Fandrick, J. J. Song, C. H. Senanayakl, *Adv. Synth. Catal.* **2011**, *353*, 1825–1864.

[2] a) J. M. Brown, in *Comprehensive Asymmetric Catalysis, Vol. 1* (Eds.: E. N. Jacobsen, A. Pfaltz, H. Yamamoto), Springer, Berlin, **1999**; b) W. Tang, X. Zhang, *Chem. Rev.* **2003**, *103*, 3029–3069; c) J.-H. Xie, S.-F. Zhu, Q.-L. Zhou, *Chem. Rev.* **2011**, *111*, 1713–1760; d) J. J. Verendel, O. Pàmies, M. Diéguez, P. G. Andersson, *Chem. Rev.* **2014**, *114*, 2130–2169.

[3] a) W. S. Knowles, M. J. Sabacky, B. D. Vineyard, *J. Chem. Soc. Chem. Commun.* **1972**, 10–11; b) W. S. Knowles, *Angew. Chem.* **2002**, *114*, 2096–2107; *Angew. Chem. Int. Ed.* **2002**, *41*, 1998–2007.

[4] R. Noyori, *Angew. Chem.* **2002**, *114*, 2108–2123; *Angew. Chem. Int. Ed.* **2002**, *41*, 2008–2022.

[5] C. S. Shultz, S. W. Krska, *Acc. Chem. Res.* **2007**, *40*, 1320–1326.

[6] H.-U. Blaser, *Adv. Synth. Catal.* **2002**, *344*, 17–31.

[7] a) X. Cui, K. Burgess, *Chem. Rev.* **2005**, *105*, 3272–3296; b) K. Källström, I. Munslow, P. G. Andersson, *Chem. Eur. J.* **2006**, *12*, 3194–3200; c) S. J.

Roseblade, A. Pfaltz, *Acc. Chem. Res.* **2007**, *40*, 1402 – 1411; d) T. L. Church, P. G. Andersson, *Coord. Chem. Rev.* **2008**, *252*, 513 – 531; e) O. Pàmies, P. G. Andersson, M. Diéguez, *Chem. Eur. J.* **2010**, *16*, 14232 – 14240; f) D. H. Woodmansee, A. Pfaltz, *Chem. Commun.* **2011**, *47*, 7912 – 7916; g) Y. Zhu, K. Burgess, *Acc. Chem. Res.* **2012**, *45*, 1623 – 1636.

[8] R. H. Crabtree, *Acc. Chem. Res.* **1979**, *12*, 331 – 337.

[9] A. Lightfoot, P. Schnider, A. Pfaltz, *Angew. Chem.* **1998**, *110*, 3047 – 3050; *Angew. Chem. Int. Ed.* **1998**, *37*, 2897 – 2899.

[10] a) J. Blankenstein, A. Pfaltz, *Angew. Chem.* **2001**, *113*, 4577 – 4579; *Angew. Chem. Int. Ed.* **2001**, *40*, 4445 – 4447; b) D.-R. Hou, J. Reibenspies, T. J. Colacot, K. Burgess, *Chem. Eur. J.* **2001**, *7*, 5391 – 5400; c) F. Menges, A. Pfaltz, *Adv. Synth. Catal.* **2002**, *344*, 40 – 44; d) M. C. Perry, X. Cui, M. T. Powell, D.-R. Hou, J. H. Reibenspies, K. Burgess, *J. Am. Chem. Soc.* **2003**, *125*, 113 – 123; e) W. Tang, W. Wang, X. Zhang, *Angew. Chem.* **2003**, *115*, 973 – 976; *Angew. Chem. Int. Ed.* **2003**, *42*, 943 – 946; f) D. Liu, W. Tang, X. Zhang, *Org. Lett.* **2004**, *6*, 513 – 516; g) S. McIntyre, E. Hörmann, F. Menges, S. P. Smidt, A. Pfaltz, *Adv. Synth. Catal.* **2005**, *347*, 282 – 288; h) M. Diéguez, J. Mazuela, O. Pàmies, J. J. Verendel, P. G. Andersson, *Chem. Commun.* **2008**, *33*, 3888 – 3890; i) M. Diéguez, J. Mazuela, O. Pàmies, J. J. Verendel, P. G. Andersson, *J. Am. Chem. Soc.* **2008**, *130*, 7208 – 7209; j) S.-M. Lu, C. Bolm, *Angew. Chem.* **2008**, *120*, 9052 – 9055; *Angew. Chem. Int. Ed.* **2008**, *47*, 8920 – 8923; k) J. Mazuela, J. J. Verendel, M. Coll, B. Schäffner, A. Börner, P. G. Andersson, O. Pàmies, M. Diéguez, *J. Am. Chem. Soc.* **2009**, *131*, 12344 – 12353; l) J. Zhao, K. Burgess, *J. Am. Chem. Soc.* **2009**, *131*, 13236 – 13237; m) W.-J. Lu, Y.-W. Chen, X.-L. Hou, *Adv. Synth. Catal.* **2010**, *352*, 103 – 107; n) Y. Zhang, Z. Han, F. Li, K. Ding, A. Zhang, *Chem. Commun.* **2010**, *46*, 156 – 158; o) A. Franzke, A. Pfaltz, *Chem. Eur. J.* **2011**, *17*, 4131 – 4144; p) J. Mazuela, P.-O. Norrby, P. G. Andersson, O. Pàmies, M. Diéguez, *J. Am. Chem. Soc.* **2011**, *133*, 13634 – 13645; q) J. Shang, Z. Han, Y. Li, Z. Wang, K. Ding, *Chem. Commun.* **2012**, *48*, 5172 – 5174; r) X. Wang, Z. Han, Z. Wang, K. Ding, *Angew. Chem.* **2012**, *124*, 960 – 964; *Angew. Chem. Int. Ed.* **2012**, *51*, 936 – 940.

[11] a) T. Bunlaksananusorn, K. Polborn, P. Knochel, *Angew. Chem.* **2003**, *115*, 4071 – 4073; *Angew. Chem. Int. Ed.* **2003**, *42*, 3941 – 3943; b) W. J. Drury III, N. Zimmermann, M. Keenan, M. Hayashi, S. Kaiser, R. Goddard, A. Pfaltz, *Angew. Chem.* **2004**, *116*, 72 – 76; *Angew. Chem. Int. Ed.* **2004**, *43*, 70 – 74; c) S. Bell, B. Wüstenberg, S. Kaiser, F. Menges, T. Netscher, A. Pfaltz, *Science* **2006**, *311*, 642 – 644; d) S. Kaiser, S. P. Smidt, A. Pfaltz, *Angew. Chem.* **2006**, *118*, 5318 – 5321; *Angew. Chem. Int. Ed.* **2006**, *45*, 5194 – 5197; e) J. Margalef, M. Lega, F. Ruffo, O. Pàmies, M. Diéguez, *Tetrahedron: Asymmetry* **2012**, *23*, 945 – 951; f) D. H. Woodmansee, M.-A. Müller, L. Tröndlin, E. Hörmann, A. Pfaltz, *Chem. Eur. J.* **2012**, *18*, 13780 – 13786; g) J. Mazuela, O. Pàmies, M. Diéguez, *Adv. Synth. Catal.* **2013**, *355*, 2569 – 2583; h) A. Schumacher, M. Bernasconi, A. Pfaltz, *Angew. Chem.* **2013**, *125*, 7570 – 7573; *Angew. Chem. Int. Ed.* **2013**, *52*, 7422 – 7425.

[12] D. Rageot, D. H. Woodmansee, B. Pugin, A. Pfaltz, *Angew. Chem.* **2011**, *123*, 9772 – 9775; *Angew. Chem. Int. Ed.* **2011**, *50*, 9598 – 9601.

[13] a) C. Hedberg, K. Källström, P. Brandt, L. K. Hansen, P. G. Andersson, *J. Am. Chem. Soc.* **2006**, *128*, 2995 – 3001; b) P. Cheruku, A. Paptchikhine, T. L. Church, P. G. Andersson, *J. Am. Chem. Soc.* **2009**, *131*, 8285 – 8289; c) P. Tolstoy, M. Engman, A. Paptchikhine, J. Bergquist, T. L. Church, A. W.-M. Leung, P. G. Andersson, *J. Am. Chem. Soc.* **2009**, *131*, 8855 – 8860; d) J. J. Verendel, J.-Q. Li, X. Quan, B. Peters, T. Zhou, O. R. Gautun, T. Govender, P. G. Andersson, *Chem. Eur. J.* **2012**, *18*, 6507 – 6513.

[14] a) K. Källström, C. Hedberg, P. Brandt, A. Bayer, P. G. Andersson, *J. Am. Chem. Soc.* **2004**, *126*, 14308 – 14309; b) J. Mazuela, A. Paptchikhine, O. Pàmies, P. G. Andersson, M. Diéguez, *Chem. Eur. J.* **2010**, *16*, 4567 – 4576.

[15] a) M. Coll, O. Pàmies, M. Diéguez, *Chem. Commun.* **2011**, *47*, 9215 – 9217; b) M. Coll, O. Pàmies, M. Diéguez, *Adv. Synth. Catal.* **2013**, *355*, 143 – 160.

[16] a) A. M. Masdeu-Bultó, M. Diéguez, E. Martin, M. Gómez, *Coord. Chem. Rev.* **2003**, *242*, 159 – 201; b) E. Martin, M. Diéguez, *C. R. Chim.* **2007**, *10*, 188 – 205; c) M. Mellah, A. Voituriez, E. Schulz, *Chem. Rev.* **2007**, *107*, 5133 – 5209; d) H. Pellissier, *Tetrahedron* **2007**, *63*, 1297 – 1330; e) R. Malacea, E. Manoury, in *Phosphorus Ligands in Asymmetric Catalysis, Vol. 2* (Ed.: A. Börner), Wiley-VCH, Weinheim, **2008**, pp. 749 – 784; f) R. Gómez Arrayás, J. C. Carretero, *Chem. Commun.* **2011**, *47*, 2207 – 2211.

[17] Thioether-phosphinite ligands **L1 d**, **L4 d**, **L6 d**, **L7 d**, and **L9 d** have been already prepared: a) X. Caldentey, M. A. Pericàs, *J. Org. Chem.* **2010**, *75*, 2628 – 2644; b) X. Caldentey, X. C. Cambeiro, M. A. Pericàs, *Tetrahedron* **2011**, *67*, 4161 – 4168.

[18] a) Y. Gao, R. M. Hanson, J. M. Klunder, S. Y. Ko, H. Masamune, K. B. Sharpless, *J. Am. Chem. Soc.* **1987**, *109*, 5765 – 5780; b) E. Medina, A. Moyano, M. A. Pericàs, A. Riera, *Helv. Chim. Acta* **2000**, *83*, 972 – 988; c) A. Vidal-Ferran, A. Moyano, M. A. Pericàs, A. Riera, *J. Org. Chem.* **1997**, *62*, 4970 – 4982.

[19] a) P. Brandt, C. Hedberg, P. G. Andersson, *Chem. Eur. J.* **2003**, *9*, 339 – 347; b) Y. Fan, X. Cui, K. Burgess, M. B. Hall, *J. Am. Chem. Soc.* **2004**, *126*, 16688 – 16689; c) X. Cui, Y. Fan, M. B. Hall, K. Burgess, *Chem. Eur. J.* **2005**, *11*, 6859 – 6868; d) T. L. Church, T. Rasmussen, P. G. Andersson, *Organometallics* **2010**, *29*, 6769 – 6781; e) K. H. Hopmann, A. Bayer, *Organometallics* **2011**, *30*, 2483 – 2497; Pfaltz's group has recently provided experimental support for a catalytic pathway going through the Ir^{III}/Ir^{V} species, see: f) S. Gruber, A. Pfaltz, *Angew. Chem.* **2014**, *126*, 1927 – 1931; *Angew. Chem. Int. Ed.* **2014**, *53*, 1896 – 1900.

[20] a) C. Lee, W. Yang, R. G. Parr, *Phys. Rev. B* **1988**, *37*, 785 – 789; b) A. D. Becke, *J. Chem. Phys.* **1993**, *98*, 5648 – 5652.

[21] a) W. J. Hehre, R. Ditchfield, J. A. Pople, *J. Chem. Phys.* **1972**, *56*, 2257 – 2261; b) P. C. Hariharan, J. A. Pople, *Theor. Chim. Acta* **1973**, *28*, 213 – 222; c) M. M. Francl, W. J. Pietro, W. J. Hehre, J. S. Binkley, M. S. Gordon, D. J. Defrees, J. A. Pople, *J. Chem. Phys.* **1982**, *77*, 3654 – 3665; d) P. J. Hay, W. R. Wadt, *J. Chem. Phys.* **1985**, *82*, 299 – 310.

[22] a) S. Miertus, J. Tomasi, *Chem. Phys.* **1982**, *65*, 239 – 245; b) B. Mennucci, J. Tomasi, *J. Chem. Phys.* **1997**, *106*, 5151 – 5158; c) M. Cossi, V. Barone, B. Menucci, J. Tomasi, *Chem. Phys. Lett.* **1998**, *286*, 253 – 260.

[23] Gaussian 09, Revision A.02, M. J. Frisch, G. W. Trucks, H. B. Schlegel, G. E. Scuseria, M. A. Robb, J. R. Cheeseman, G. Scalmani, V. Barone, B. Mennucci, G. A. Petersson, H. Nakatsuji, M. Caricato, X. Li, H. P. Hratchian, A. F. Izmaylov, J. Bloino, G. Zheng, J. L. Sonnenberg, M. Hada, M. Ehara, K. Toyota, R. Fukuda, J. Hasegawa, M. Ishida, T. Nakajima, Y. Honda, O. Kitao, H. Nakai, T. Vreven, J. A. Montgomery, J. E. Peralta, Jr., F. Ogliaro, M. Bearpark, J. J. Heyd, E. Brothers, K. N. Kudin, V. N. Staroverov, R. Kobayashi, J. Normand, K. Raghavachari, A. Rendell, J. C. Burant, S. S. Iyengar, J. Tomasi, M. Cossi, N. Rega, J. M. Millam, M. Klene, J. E. Knox, J. B. Cross, V. Bakken, C. Adamo, J. Jaramillo, R. Gomperts, R. E. Stratmann, O. Yazyev, A. J. Austin, R. Cammi, C. Pomelli, J. W. Ochterski, R. L. Martin, K. Morokuma, V. G. Zakrzewski, G. A. Voth, P. Salvador, J. J. Dannenberg, S. Dapprich, A. D. Daniels, Ö. Farkas, J. B. Foresman, J. V. Ortiz, J. Cioslowski, D. J. Fox, Gaussian, Inc., Wallingford CT, **2009**.

[24] a) R. Krishnan, J. S. Binkley, R. Seeger, J. A. Pople, *J. Chem. Phys.* **1980**, *72*, 650; b) A. D. McLean, G. S. Chandler, *J. Chem. Phys.* **1980**, *72*, 5639 – 5648.

[25] a) S. Grimme, J. Antony, S. Ehrlich, H. Krieg, *J. Chem. Phys.* **2010**, *132*, 154104; b) S. Grimme, S. Ehrlich, L. Goerigk, *J. Comput. Chem.* **2011**, *32*, 1456 – 1465.

[26] The additional isomers generated considering the hydride attack to the less-substituted carbon of the olefin have not been considered, since it has been previously demonstrated that they have substantially higher energies. See ref. [19d].

[27] Unpublished results. In all cases, enantioselectivities were below 50% *ee*.

[28] W.-J. Lu, X.-L. Hou, *Adv. Synth. Catal.* **2009**, *351*, 1224 – 1228.

[29] a) A. Paptchikhine, P. Cheruku, M. Engman, P. G. Andersson, *Chem. Commun.* **2009**, 5996 – 5998; b) A. Ganić, A. Pfaltz, *Chem. Eur. J.* **2012**, *18*, 6724 – 6728.

[30] a) K. Oertel, G. Zech, H. Kunz, *Angew. Chem.* **2000**, *112*, 1489 – 1491; *Angew. Chem. Int. Ed.* **2000**, *39*, 1431 – 1433; b) A. Fürstner, M. Bindl, L. Jean, *Angew. Chem.* **2007**, *119*, 9435 – 9438; *Angew. Chem. Int. Ed.* **2007**, *46*, 9275 – 9278; c) J. Li, J. Dai, X. Chen, P. Zhu, *J. Nat. Prod.* **2007**, *70*, 1846 – 1849; d) A. M. McGhee, J.-C. Kizirian, D. J. Procter, *Org. Biomol. Chem.* **2007**, *5*, 1021 – 1024.

[31] a) G. W. Kabalka, *J. Organomet. Chem.* **1984**, *274*, 1 – 29; b) G. W. Kabalka, R. C. Marks, *J. Organomet. Chem.* **1993**, *457*, 25 – 40; c) J. B. Morgan, J. P. Morken, *J. Am. Chem. Soc.* **2004**, *126*, 15338 – 15339; d) W. J. Moran, J. P. Morken, *Org. Lett.* **2006**, *8*, 2413 – 2415.

[32] This behavior has been explained by the strong polarization of the double bond in these α,β-unsaturated compounds. For α,β-disubstituted substrates the addition to the β-C is hampered by steric interactions caused by the olefin tilting toward the ligand bulk, whereas addition to the α-C is electronically disfavored. Since the quadrant model relies on

steric effects, the failure of the model for α,β-disubstituted substrates indicates that electronic factors dominate. See, also: J.-Q. Li, X. Quan, P. G. Andersson, *Chem. Eur. J.* **2012**, *18*, 10609 – 10616.

[33] The flexibility of the biphenyl moiety has been demonstrated to be crucial in the success of ligands containing this moiety in several catalytic reactions. For a recent review, see: P. W. N. M. van Leeuwen, P. C. Kamer, C. Claver, O. Pàmies, M. Diéguez, *Chem. Rev.* **2011**, *111*, 2077 – 2118.

[34] The same can be achieved with thioether-phosphinite ligands by changing the absolute configuration of the starting enantiopure epoxide.

[35] Unpublished results. The use of previously reported furanoside-based P–S ligands led to moderate enantioselectivities.

[36] a) M. Schlosser, *Angew. Chem.* **1998**, *110*, 1538 – 1556; *Angew. Chem. Int. Ed.* **1998**, *37*, 1496 – 1513; b) P. V. Ramachandran, *Asymmetric Fluoroorganic Chemistry: Synthesis Application and Future Directions*, Washington, **2000**; c) B. E. Smart, *J. Fluorine Chem.* **2001**, *109*, 3 – 11; d) A special issue has been devoted to *Fluorine in the Life Sciences*: *ChemBioChem* **2004**, *5*, 559 – 562.

[37] PC is a noncorrosive, nonhygroscopic, high boiling, nontoxic, and biodegradable solvent.

[38] a) J. Bayardon, J. Holz, B. Schäffner, V. Andrushko, S. Verevkin, A. Preetz, A. Börner, *Angew. Chem.* **2007**, *119*, 6075 – 6078; *Angew. Chem. Int. Ed.* **2007**, *46*, 5971 – 5974; b) B. Schäffner, F. Schäffner, S. P. Verevkin, A. Börner, *Chem. Rev.* **2010**, *110*, 4554 – 4581.

[39] S. P. Smidt, A. Pfaltz, E. Martínez-Viviente, P. S. Pregosin, A. Albinati, *Organometallics* **2003**, *22*, 1000 – 1009.

[40] G. J. H. Buisman, P. C. J. Kamer, P. W. N. M. van Leeuwen, *Tetrahedron: Asymmetry* **1993**, *4*, 1625 – 1634.

[41] T. Ohta, H. Ikegami, T. Miyake, H. Takaya, *J. Organomet. Chem.* **1995**, *502*, 169 – 176.

[42] D. H. Woodmansee, M.-A. Müller, M. Neuburger, A. Pfaltz, *Chem. Sci.* **2010**, *1*, 72 – 78.

[43] K. Källström, I. J. Munslow, C. Hedberg, P. G. Andersson, *Adv. Synth. Catal.* **2006**, *348*, 2575 – 2578.

[44] S. Deerenberg, P. C. J. Kamer, P. W. N. M. van Leeuwen, *Organometallics* **2000**, *19*, 2065 – 2072.

Received: April 6, 2014
Published online on August 5, 2014